A fiber-optic chemical sensor based on surface plasmon resonance

R. C. Jorgenson and S. S. Yee

Sensor Technology Research Group, Department of Electrical Engineering, University of Washington, Seattle, WA 98195 (USA)

(Received September 23, 1992; in revised form December 15, 1992; accepted December 20, 1992)

Abstract

A fiber-optic chemical sensor is presented which utilizes surface plasmon resonance excitation. The sensing element of the fiber has been fabricated by removing a section of the fiber cladding and symmetrically depositing a thin layer of highly reflecting metal onto the fiber core. A white-light source is used to introduce a range of wavelengths into the fiber optic. Changes in the sensed parameters (e.g., bulk refractive index, film thickness and film refractive index) are determined by measuring the transmitted spectral-intensity distribution. Experimental results of the sensitivity and the dynamic range in the measurement of the refractive indices of aqueous solutions are in agreement with the theoretical model of the sensor.

1. Introduction

Many optical sensing systems have been developed utilizing the sensitivity of surface plasmon resonance (SPR) to the refractive indices of bulk and thin-film dielectrics and to the thicknesses of thin films. These sensing systems in conjunction with the appropriate chemically sensitive layers have allowed researchers to develop a variety of SPR-based chemical sensors, including immunoassay [1–3], gas [1, 4], and liquid sensors [5]. One such chemical-sensing system has been commercialized by Pharmacia (Uppsala, Sweden). However, all these systems utilize bulk-optic configurations that are limited by the use of a coupling prism. The resulting systems are relatively large and expensive and are also inapplicable for remote sensing applications.

Traditionally, SPR is measured using the Kretschmann configuration, illustrated in Fig. 1, with a prism and a thin highly reflecting metal layer (e.g., silver or gold) deposited upon the prism base [6]. The SPR reflection spectrum (reflected light intensity versus angle of incidence with respect to the normal of the metal/dielectric interface) is measured by coupling transverse magnetically (TM) polarized monochromatic light into the prism and measuring the reflected light intensity of the ray exiting the prism versus the angle of incidence. An example of the resultant theoretical spectrum is illustrated in Fig. 2. The angle at which the minimum reflection intensity occurs, θ_{sp}, is the resonance angle at which coupling of energy occurs between the incident light and the surface plasmon waves.

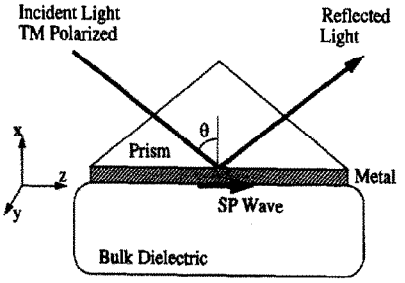

Fig. 1. The Kretschmann configuration.

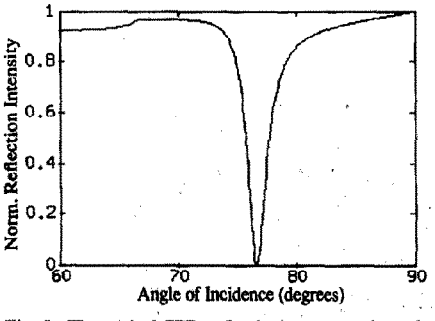

Fig. 2. Theoretical SPR reflection spectrum for a bulk dielectric of water, a wavelength of 620 nm, a 550 Å thick silver film, and a fused silica prism.

A novel fiber-optic SPR sensing configuration without the required light-coupling prism is presented. This sensing configuration allows for a small sensing element and sample volume, simplified optical design, potential use for disposable fiber-optic sensors and the capability for remote sensing.

0925-4005/93/$6.00

The sensing element is a segment of fiber in which the cladding has been removed and a 550 Å thick silver film has been symmetrically deposited on the fiber core, via electron-beam evaporation. The length of the cladding removed was calculated to optimize the average number of reflections for all the propagating rays of light in the fiber. Unlike traditional SPR measurements, which employ a discrete excitation wavelength while modulating the angle of incidence, the SPR fiber-optic sensor system uses a white-light source, resulting in a large range of excitation wavelengths. The range of incident angles is limited to only those angles that propagate in the optical fiber. The sensed parameters can then be determined from the measured resonance spectrum in the transmitted spectral intensity distribution.

2. Theory

2.1. Background

SPR is a resonance phenomenon in which surface plasmon waves (SPWs) are excited at a metal/dielectric interface. The electric field, $\boldsymbol{E}$, of the SPW propagating in the z-direction (Fig. 1) is expressed as [7]

$$\boldsymbol{E}_x(x, z, t) = E_x^0(x) \exp(i\omega t - ik_z z) \tag{1}$$

where ω = angular frequency and

$$k_z = k_z' + ik_z''$$

is the SPR propagation constant along the z-direction.

The SPR propagation constant, k_z, is dependent upon the free-space wave number, k_0, and the complex permittivities of the metal, ε_m, and the dielectric, ε_d. The propagation constant is expressed as

$$k_z = k_0 \left(\frac{\varepsilon_m \varepsilon_d}{\varepsilon_m + \varepsilon_d} \right)^{1/2} \tag{2}$$

At the resonance angle θ_{sp}, the propagation constant of the incident beam parallel to the prism base (i.e., along the z-direction, $k_0 n_p \sin \theta_{sp}$) is equal to the real part of the SPR propagation constant. This equality condition is expressed by

$$k_z' = k_0 n_p \sin \theta_{sp} \tag{3}$$

where n_p is the refractive index of the prism.

Equations (2) and (3) provide for the theoretical transduction mechanism for SPR as a sensor. Specifically, an increase in refractive index of the sensed dielectric will cause a shift in the resonance spectrum toward larger SPR coupling angles. By measuring the SPR resonance parameters (coupling angle, θ_{sp}, full width at half maximum, $\Delta\theta$, and the reflected light intensity at the resonance coupling angle, R_{min}) one can determine the complex refractive index of the dielectric using the calculated SPR propagation constant, k_z [8].

The SPR reflection spectrum in Fig. 2 is for a discrete wavelength. For other excitation wavelengths the SPR propagation constant will change accordingly, since the prism refractive index, bulk dielectric refractive index and the metal permittivity are all a function of wavelength [9]. A theoretical three-dimensional SPR reflection spectrum for a range of wavelengths is illustrated in Fig. 3 with the value of one minus the normalized reflected intensity versus the angle of incidence and

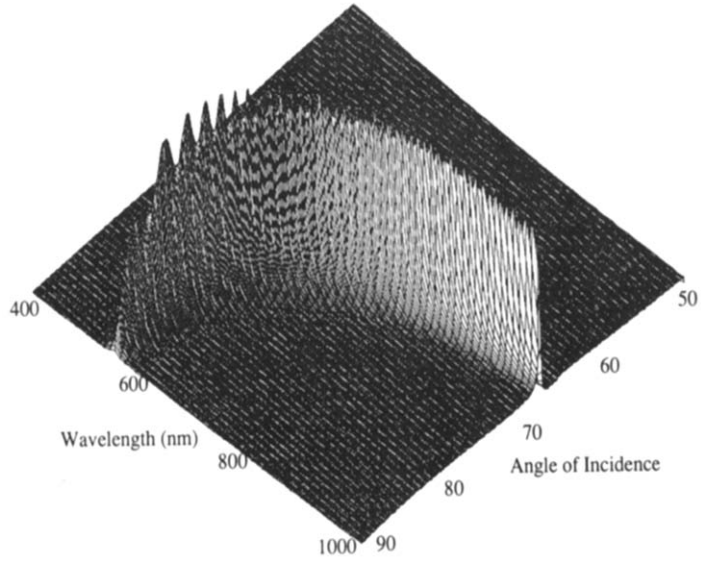

Fig. 3. Theoretical three-dimensional SPR reflection spectra for a bulk dielectric of water, a 550 Å thick silver film, and a fused silica prism. The unlabelled axis is equal to 1−normalized reflection intensity.

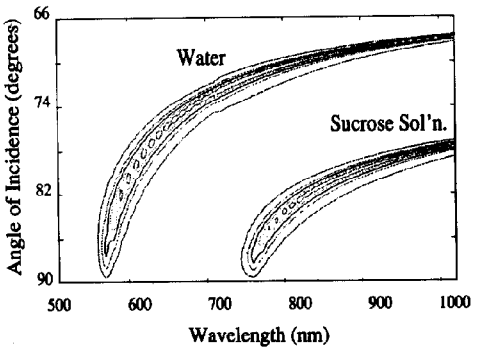

Fig. 4. The set of curves labeled 'Water' is the contour plot of the three-dimensional SPR spectra illustrated in Fig. 3. The set of curves labeled 'Sucrose Sol'n' is the contour plot of the theoretical spectra assuming a 37.1% concentration of sucrose.

wavelength. Note that the discrete peaks in Fig. 3 correspond to the use of discrete data points in order to create the graph. However, in theory the three-dimensional surface is actually a continuous peaked surface. The spectrum was calculated using a matrix method to determine the Fresnel reflection coefficients of a multilayered structure [10]. The calculations were made assuming a fused silica prism, a 550 Å thick silver layer, a bulk dielectric of water, and TM-polarized light. The refractive-index values used in our SPR spectra calculations for the silver layer [11], fused silica prism [12], and water [13] were obtained from the literature. The change in the SPR coupling angle as a function of wavelength shown in Fig. 3 is almost exclusively due to the increased magnitude of the silver complex refractive index over the wavelength range 400–1000 nm. This large change in the silver refractive index (i.e., one order of magnitude) is compared to the relatively small change in both silica and water refractive indices, 0.019 and 0.028 index of refraction units, respectively.

Figure 4 is a contour plot of two theoretical three-dimensional SPR reflection spectra for water and a sucrose solution (37.1 wt.%) as the bulk dielectric media. This plot illustrates the resonance coupling angle dependency upon wavelength, and the three-dimensional SPR spectra dependence upon the bulk refractive index. It is clear from Fig. 4 that a very sharp resonance would be observed at the longer-wavelength region for the fused silica prism and silver metal layer configuration. Thus, it explains why many researchers involved in SPR sensing have employed the method of fixed wavelength and modulated angle of incidence at long wavelengths. These contour plots illustrate that it is also possible to measure a resonance spectrum by the method of fixing the angle of incidence and modulating the excitation wavelength, which is the fundamental basis for the development of the SPR fiber-optic sensor.

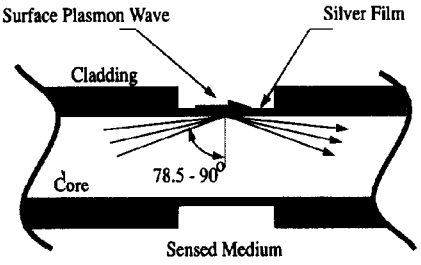

Fig. 5. Illustration of the SPR fiber-optic sensing element.

2.2. Principle of the SPR fiber-optic sensor

The SPR sensor has eliminated the need for the coupling prism by depositing the metal directly onto the core of the fiber as illustrated in Fig. 5. The SPR sensing method of fixed angle of incidence and modulated wavelength was selected since the wavelength intensity distribution may be preserved in a fiber optic, whereas the angular intensity distribution of light will be indistinguishable due to mode mixing as a result of the inherent bending of the multimode fiber optic in practical sensing applications. Furthermore, since the sensor is fabricated on a multimode fiber there is not a fixed angle of incidence, but rather a range of incident angles that are allowed to propagate in the fiber.

The multimode fiber optic has a numerical aperture of 0.36. The fiber supports internal propagating angles of light from 90.0 to 78.5°, with respect to the normal of the core/cladding interface. Within this incident angular region the predicted SPR coupling wavelengths are between 560 and 620 nm for a bulk dielectric of water, as shown in Fig. 4. Thus the light intensity at these wavelengths is expected to be attenuated due to the excitation of surface plasmon waves at the silver film/bulk dielectric interface. An optical system required for this fiber-optic sensor must have the capability for coupling a wide range of optical wavelengths into the optical fiber and for measuring the transmitted spectral intensity distribution (intensity versus wavelength) at the output of the fiber.

2.3. Modeling of the fiber-optic signal

Three considerations must be addressed in order to model the theoretical SPR fiber-optic sensor transmitted spectral intensity distribution. These considerations are: (1) the three-dimensional SPR reflection spectra; (2) the number of reflections each propagating mode undergoes; (3) the density of propagating modes in the fiber-optic sensor.

Figure 6 illustrates the theoretical SPR spectra of reflected intensity for one reflection versus wavelength for a number of angles propagating inside the fiber-optic sensor (90, 87, 84, 81, and 78° with respect to the normal of the core/metal interface). However, the number of

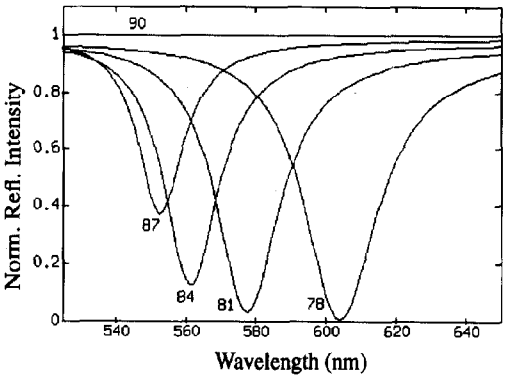

Fig. 6. Theoretical SPR spectra of reflected light intensity vs. wavelength for a number of angles propagating inside the fiber-optic sensor, i.e., 90, 87, 84, 81, and 78°. These spectra assume a core material of fused silica, bulk dielectric of water, a 550 Å silver film and TM polarization of the light.

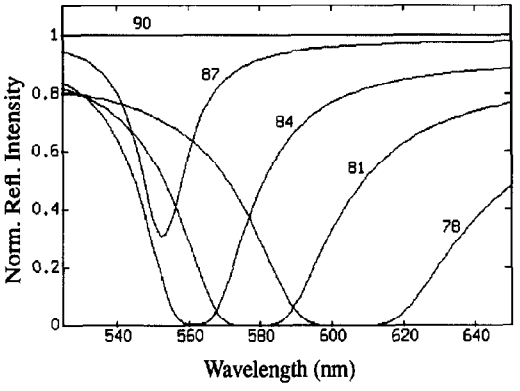

Fig. 7. Theoretical SPR spectra taking into account the number of reflections each angle encounters.

reflections in the fiber-sensor area is a function of the mode propagation angle, θ, as well as of the diameter of the fiber, d, and the length of the sensing area, L. This relationship is given by

$$\text{Number of reflections} = \frac{L}{d\tan(\theta)} \tag{4}$$

The calculated numbers of reflections for the angles propagating in the fiber are 0.00, 1.31, 2.63, 3.96, and 5.31 for incident angles of 90, 87, 84, 81, and 78°, respectively. The number of reflections was calculated assuming a 400 μm fiber diameter and a sensing area length of 10 mm.

To determine the effective SPR spectra (taking into account multiple reflections), the spectrum for a single reflection (Fig. 6) is raised to the power of the number of reflections the specific propagating angle undergoes with the sensor interface. Figure 7 illustrates these effective SPR spectra of intensity versus wavelength for

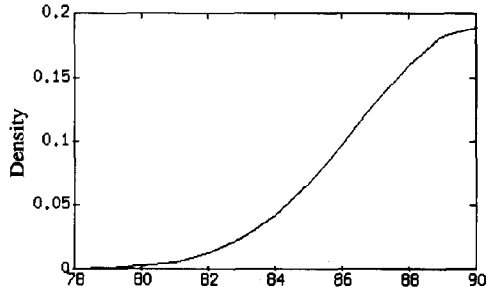

Fig. 8. Mode density as a function of incident angle, calculated assuming a Gaussian distribution of propagating angles of incidence within the fiber-optic SPR sensor.

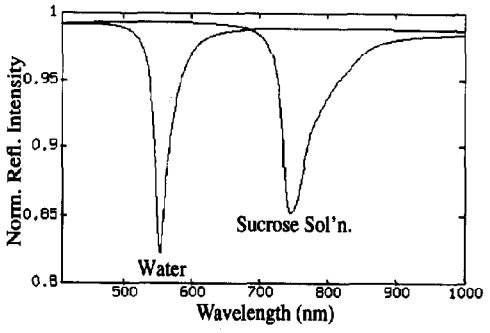

Fig. 9. Theoretical SPR fiber-optic spectra for a bulk refractive index of water and a 37.1% sucrose solution, assuming random polarized light.

five of the propagating angles. The spectrum with the lowest-order mode, 90° angle of propagation, travels parallel to the meridonial axis of the fiber and does not reflect off the interface. Therefore, the expected spectrum is that of the 90° spectrum in Fig. 6 raised to the power of zero, which yields a constant spectrum corresponding to no surface plasmon waves excited by the 90° propagating mode. Correspondingly, the smallest propagating angle in the fiber (78°) has an effective spectrum that is greatly broadened since it has 5.31 reflections within the sensing length of the sensor.

The SPR fiber-optic signal represents an accumulated spectrum for the entire range of propagating angles, since one cannot measure the SPR spectrum for a specific mode. However, the signal is not an equally weighted average of all the angles propagating in the fiber; it must be weighted with the non-constant density-distribution function of propagating angles in the fiber (Fig. 8). The propagation angle density-distribution function is assumed to be Gaussian, spanning the range of the allowed propagating angles in the fiber. Figure 9 represents the theoretical SPR fiber-optic signal obtained by weight averaging the angular spectra in Fig. 7 with the density distribution of Fig. 8 for the bulk chemical water sample and a 37.1% concentration of

sucrose. An approximate 200 nm shift in the SPR coupling wavelength is observed; it corresponds to a change of 0.06 index of refraction units of the chemical sample.

3. Experimental

The block diagram of the experimental set-up is shown in Fig. 10. The output of a tungsten–halogen lamp is focused into a fiber optic. An SPR sensing surface has been fabricated in the middle section of the length of fiber. A mode scrambler is used to populate all the modes of the fiber optic. The SPR sensing surface is enclosed by a 3 ml flow cell constructed using a syringe with two syringe stoppers and inlet and outlet ports. The output of the fiber-optic sensor is connected to a fiber-optic spectrograph (American Holographic, Littleton, MA) via an SMA connector. The flat field grating is an American Holographic model # 446.33, which disperses a range of wavelengths from 400 to 900 nm with a linear dispersion value of 20 nm/mm. The detector inside the spectrograph is a 1024-element CCD linear array detector. The theoretical wavelength resolution determined by the linear dispersion value of the grating and the 25.4 μm width of the CCD elements is 0.5 nm. A data-acquisition board is used with an IBM-compatible computer for automated data acquisition.

The fiber optic chosen for the experiment was a silica/polymer fiber (3M, Minneapolis, MN, type FP-400 UHT). The 400/600/760 μm (core, cladding and buffer diameters, respectively) fiber had a numerical aperture of 0.36. The buffer and cladding layers were removed using a technique employed by Weber and Schultz [14]. A hobby torch was used to burn away the layers, and the resultant surface was wiped with Dynasolve 100 (Dynaloy Inc.).

Three fiber-optic sensors were fabricated by removing 6, 10, and 18 mm in length of the cladding/buffer layers. The sensors were then mounted in an electron-beam evaporator system in an arrangement whereby the flux of the evaporated metal was perpendicular to the axis of the fiber. The fibers were then rotated during silver deposition, resulting in a 550 Å silver film deposited symmetrically about the fiber core. The deposition process was monitored using a quartz-crystal detector.

Six sample solutions of high-fructose corn syrup diluted with deionized water were prepared, resulting in various real refractive indices. The real refractive indices of these sample solutions (1.333, 1.351, 1.364, 1.381, 1.393, and 1.404) were independently measured using an Abbe refractometer (Milton Roy Tabletop Refractometer 3L) at the 589 nm wavelength. The same experimental procedure was used for measuring the transmitted fiber-optic SPR spectra in all three sensors. First, the transmitted spectral intensity distribution was measured while air was in the flow cell. Secondly, the transmitted spectral intensity distribution was measured for each of the six prepared sucrose solutions. 15 ml of each sample solution was introduced via a syringe at the input port of the flow cell.

4. Experimental results and discussion

The air spectrum was used as a reference to normalize all the SPR fiber-optic sensor spectra taken of the sample solutions, since there was no surface plasmon resonance excitation in this wavelength range for the bulk refractive index of air, 1.0. This calibration provided an effective means to measure the system transfer function, attributed by the light-source spectral output, the photodiode array spectral sensitivity, and the fiber spectral absorbance. Figure 11 shows the normalized transmitted light intensity as a function of wavelength measured by the 10 mm exposed core sensor for the fructose solutions with refractive indices of 1.351, 1.393, and 1.404. The resonance wavelength shift for increas-

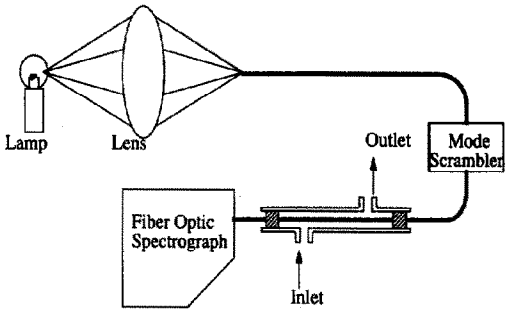

Fig. 10. Illustration of the SPR fiber-optic experimental apparatus.

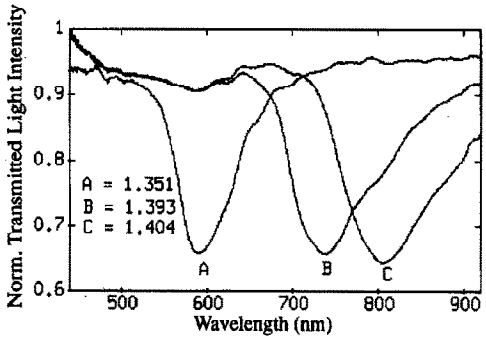

Fig. 11. SPR spectra collected using the SPR fiber sensor with 10 mm of fiber core exposed. The spectra were collected from fructose samples with refractive indices of 1.351, 1.393, and 1.404.

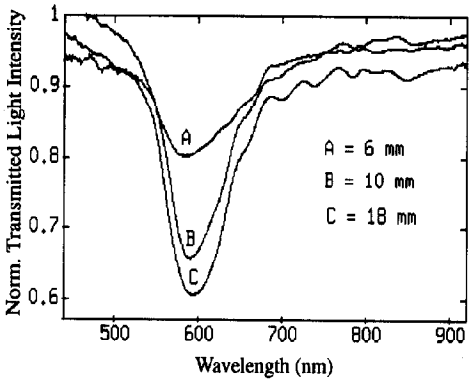

Fig. 12. SPR spectra collected from all three fabricated sensors with the same fructose concentration with a refractive index of 1.351.

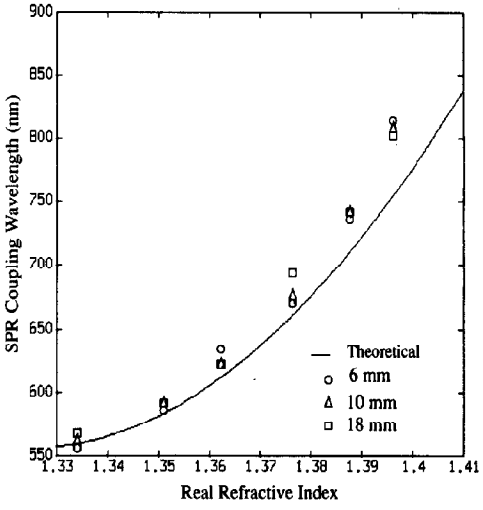

Fig. 13. Experimental and theoretical SPR fiber-optic coupling wavelength response as a function of the refractive index of the chemical sample.

ing bulk refractive indices was consistent with the theoretical results illustrated in Fig. 9. However, the resonance spectra appear to be broader than expected. This may be partly attributed to the fact that the input fiber to the fiber-optic spectrograph is large, 400 μm, and thus the full spectrograph resolution is not optimized. Narrower resonance spectra may be achieved by reducing the diameter of the input fiber to the spectrograph or by employing a narrow slit.

Figure 12 is a plot of the SPR fiber-optic sensor spectra measured by the 6, 10, and 18 mm exposed core sensors for a single fructose solution. The transmitted spectral-intensity distribution depends upon the length of SPR sensing area. As shown in Fig. 12, the spectrum measured by a longer sensing area exhibits a deeper resonance for the reasons discussed in Section 2.3. It should be noted that due to the cylindrical geometry of the fiber, both TE- and TM-polarized light with respect to the core/metal interface are allowed to propagate in the multimode fiber optic. The expected optimal transmitted light intensity at resonance is 0.50 rather than 0.0, since SPR can only be excited with TM-polarized light.

The theoretical and experimental SPR coupling wavelength versus the refractive index of the fructose sample solutions are plotted in Fig. 13 for all three SPR fiber-optic sensors. The response of all three sensors is in good agreement with the calculated values. In order to plot the Abbe refractometer measured refractive indices of the sample solutions in Fig. 13, the values were corrected for wavelength using the refractometer dispersion measurement table [15]. The theoretical sensitivity of the fiber-optic SPR sensor to refractive index can be calculated from the SPR wavelength response curve. Because the response is non-linear, the sensitivity will be a function of wavelength, with better sensitivity at the longer wavelengths. The theoretical sensitivity to refractive index is 2.5×10^{-4} at a wavelength of 500 nm and 7.5×10^{-5} at a wavelength of 900 nm, assuming the optimal wavelength resolution of the spectrograph is 0.5 nm.

The experimental results presented verify the sensing mechanism of the surface-plasmon-resonance-based fiber-optic sensor. Currently, we are directing our effort toward the optimization of the fiber sensor, taking into consideration type of metal, length of sensing area, fiber-optic core material, numerical aperture, and fiber diameter, as well as a new sensing head for possible disposable sensing applications.

5. Improved sensor and system design

An improved sensor and system configuration has been developed that has many advantages for practical chemical-sensing applications, including: (1) elimination of flow-cell limitations; (2) the possibility of disposable fiber-sensor probes; (3) amenable for use in remote sensing applications. The improved sensor and system design, illustrated in Fig. 14, utilizes a terminated sensor. This terminated reflection-based SPR fiber-optic sensor is based on the same principles as the in-line transmission-based sensor. However, the terminated sensor design utilizes a microfabricated mirror at the end of the probe to reflect the light back through the fiber. In this configuration the light travels through the sensing area twice, thus the sensing length must be one half the length of the sensing area of the in-line transmission-based sensor.

In the improved sensor configuration light is coupled into a single branch of a 50:50 two-way fiber-optic

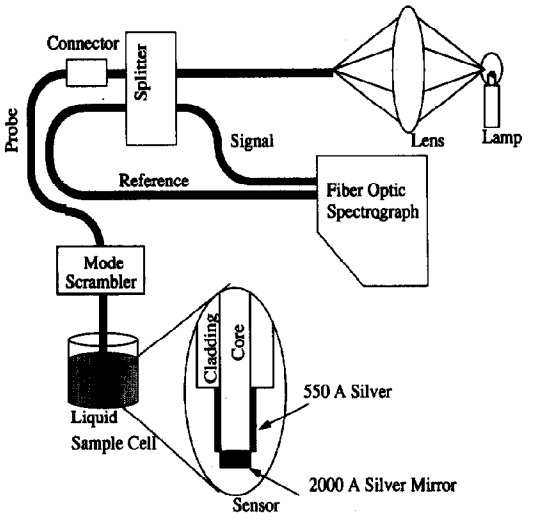

Fig. 14. Illustration of the SPR fiber-optic sensor and sensor system.

splitter from a tungsten–halogen lamp. 50% of the coupled light is then transferred to the probe branch of the splitter. An SMA connector is used to connect the splitter to the disposable SPR fiber-optic sensor probe. The light is transmitted down the probe to the sensor area and reflected back up the probe by the use of a microfabricated mirror. The returned light is split again and connected to a fiber-optic spectrograph, which is used to measure the spectral intensity of the signal light. A reference signal can also be measured by use of the remaining splitter arm.

The results obtained from the reflected sensor configuration are consistent with the data and theory of the in-line transmission-based SPR fiber-optic sensor presented in this paper.

6. Conclusions

A fiber-optic SPR sensor has been presented that utilizes the sensitivity of surface plasmon resonance combined with fiber-optic technology. The sensor signal and response were theoretically modelled and the optimal sensitivity was found to be between 4.5×10^{-4} and 7.5×10^{-5} index of refraction units. This is comparable to the sensitivity of traditional SPR bulk-optic systems. The sensing principle of the device was based upon fixed angle of incidence and modulated wavelength measurements, instead of the more traditional fixed wavelength and modulated angle of incidence measurements used in bulk-optic SPR systems.

The measured responses of the sensing probes were in good agreement with the theoretical model. The fiber-optic SPR sensing probes (capable of remote and *in situ* monitoring) will likely be developed toward applications in process analytical chemistry, environmental monitoring, and biochemical and biomedical sensing.

Acknowledgements

The authors wish to thank Frank Lawrence for his assistance in the sensor fabrication, fructose solution preparation, and data acquisition. We also thank Dr Lloyd Burgess, Dr Martin Afromowitz and Kevin Kuhn for their helpful discussions, Dr Robert Darling for use of his electron-beam evaporation system, and Kyle Johnston for his assistance in fabricating the 'reflected' sensor configuration. This work is supported by the Center for Process Analytical Chemistry (CPAC) an NSF/Industry Cooperative Research Center at the University of Washington and an NSF grant, # EID-9212314.

References

1 B. Liedberg, C. Nylander and I. Lundström, Surface plasmon resonance for gas detection and biosensing, *Sensors and Actuators, 4* (1983) 299–304.
2 P. B. Daniels, J. K. Deacon, M. J. Eddowes and D. Pedley, Surface plasmon resonance applied to immunosensing, *Sensors and Actuators, 15* (1988) 11–17.
3 R. C. Jorgenson, S. S. Yee, K. K. Chittur and L. W. Burgess, *In-situ* characterization of adsorbed protein films using surface plasmon resonance, *IEEE/Eng. Medicine Biology Soc. Proc.*, Vol. 12, 1990, pp. 440–442.
4 J. Gent, P. Lambeck, H. Kreuwel, G. Gerritsma, E. Sudholter, D. Reinhoudt and J. Popma, Optimization of the chemooptical surface plasmon resonance based sensor, *Appl. Opt., 29* (1990) 2843–2849.
5 K. Matsubaru, S. Kawata and S. Minami, Optical chemical sensor based on surface plasmon measurement, *Appl. Opt., 27* (1988) 1160–1163.
6 E. Kretschmann and H. Raether, Radiative decay of non-radiative surface plasmons excited by light, *Z. Naturforsch., Teil A, 23* (1968) 2135–2136.
7 J. Gent, P. Lambeck, H. Kreuwel, G. Gerritsma, E. Sudholter, D. Reinhoudt and J. Popma, Chromoionophores in optical ion sensors, *Sensors and Actuators, 17* (1989) 297–305.
8 E. Fontana, R. H. Pantell and M. Moslehi, Characterization of dielectric-coated, metal mirrors using surface plasmon spectroscopy, *Appl. Opt., 27* (1988) 3334–3339.
9 R. Jorgenson, Surface plasmon resonance as an optical probe of the metal/dielectric interface, *Master's Thesis*, University of Washington, 1991.
10 C. Jung, Surface plasmon resonance, *Master's Thesis*, University of Washington, 1991.
11 G. Hass and L. Hadley, Optical properties of metals, in D. Gray (ed.), *American Institute of Physics Handbook*, McGraw-Hill, New York, 1972, pp. 149–151.
12 M. Querry, D. Wieliczka and D. Segelstein, Water (H_2O), in E. Palik (ed.), *Handbook of Optical Constants of Solids II*, Academic Press, Boston, 1991, pp. 1059–1077.

13 I. H. Malitson, Interspecimen comparison of the refractive index of fused silica, *J. Opt. Soc. Am.*, *55* (1965) 1205–1216.
14 A. Weber and J. S. Schultz, Fiber-optic fluorimetry in biosensors: comparison between evanescent wave generation and distal-face generation of fluorescent light, *Biosensors Bioelectron.*, 7 (1992) 193–197.
15 *Abbe Refractometer Operator's Manual and Dispersion Table*, Milton Roy Company, Analytical Products Division, Rochester, New York, 1986.

Biographies

Ralph C. Jorgenson received B.S. and M.S. degrees in electrical engineering from the University of Washington in 1988 and 1991, respectively. He is currently a Ph.D. candidate in the Department of Electrical Engineering at the University of Washington. He has interned at International Biomedics Inc. (1986), researching an *in vivo* fiber-optic blood-gas sensor and at Battelle Memorial Institute (1987, 1988) investigating bulk-optic surface plasmon resonance for the measurement of *in situ* protein adsorption. His main research interests are in chemical and biomedical optical sensors.

Sinclair S. Yee received B.S., M.S., and Ph.D. degrees in electrical engineering from the University of California, Berkeley, in 1959, 1961, and 1965, respectively. In 1964, he joined the Lawrence Livermore Laboratory as a research engineer working on semiconductor devices. Since 1966 he has been on the faculty of the Department of Electrical Engineering at the University of Washington, where in 1974 he became a full professor. In 1972–1974, he was an NIH Special Research Fellow, and since 1979, he has been an IEEE Fellow. His main research interests are concerned with silicon-based and GaAs quantum-well optical modulator devices and surface plasmon resonance, as well as microsensor arrays.